Drug Design, Development and Therapy

Dovepress
Taylor & Francis Group

Open Access Full Text Article

ORIGINAL RESEARCH

# Astragaloside IV Alleviates Systemic Lupus Erythematosus by Modulating ITGB1/PTK2/p38 Pathway: Integrated Network Pharmacology and Experimental Validation

Zhongfu Tang, Lili Cheng, Ming Li, Chuanbing Huang

Department of Rheumatology, The First Affiliated Hospital of Anhui University of Traditional Chinese Medicine, Hefei, People's Republic of China

Correspondence: Chuanbing Huang, Department of Rheumatology, The First Affiliated Hospital of Anhui University of Traditional Chinese Medicine, No. 117 Meishan Road, Shushan District, Hefei, Anhui, People's Republic of China, Email chuanbingh@ahtcm.edu.cn



**Purpose:** Systemic lupus erythematosus (SLE) features immune cell dysfunction, causing immune - complex and inflammatory - factor formation that damages organs. Astragaloside IV (AS-IV), a cyclic triterpene saponin from Astragalus membranaceus, has strong anti-inflammatory and immunomodulatory effects. This study aimed to evaluate AS-IV's therapeutic potential for SLE and uncover its mechanism.

**Methods:** MRL/lpr mice were divided into MRL/lpr, low - medium - high - dose AS-IV, and Pred groups, with C57BL/6 mice as controls. Renal damage was assessed by histopathology and electron microscopy. Immune parameters were analyzed using ELISA, flow cytometry, immunofluorescence, and immunohistochemistry. Network pharmacology was used to find AS-IV's SLE targets, and molecular docking was employed to clarify its mechanism, with multiple methods used to measure target expression.

**Results:** AS-IV ameliorated renal pathology by reducing glomerular and vascular wall lesion scores while attenuating immune complex deposition. It significantly decreased podocyte foot process fusion rates, alleviated overall renal damage, and reduced key renal inflammatory cytokines. Systemically, AS-IV reduced spleen index and lowered anti-dsDNA, IgG levels, while restoring complement components C3 and C4, akin to the effects observed in the Pred group. AS-IV notably downregulated the expression of ITGB1, PTK2, p38, IL-4, IL-21, IL-17, and the Th1/Th2 and Th17 ratios, while upregulating the Treg ratio compared to the MRL/lpr group. Molecular docking and Western blot analyses further validated the interaction between AS-IV and the ITGB1/PTK2/p38 axis.

**Conclusion:** AS-IV can modulate the ITGB1/PTK2/p38 axis to suppress immune inflammatory responses, thereby ameliorating SLE progression. These findings suggest the certain therapeutic value of AS-IV in managing SLE.

**Keywords:** astragaloside IV, systemic lupus erythematosus, immune function, inflammatory factors, network pharmacology

## Introduction

Systemic Lupus Erythematosus (SLE) is a chronic autoimmune disease characterized by the production of autoantibodies, inflammatory damage to multiple organs, and disruption of immune tolerance mechanisms.[1] The pathogenesis involves intricate networks of interactions, including genetic predisposition, aberrant epigenetic modifications, immune cell dysfunction, and imbalances in cytokine microenvironments.[2] Growing evidence suggests that T cell and B cell dysfunction are pivotal in SLE pathogenesis,[3] particularly the aberrant differentiation of T cells and the resulting increase in plasma cells, which are considered crucial drivers of disease progression.[4] Epidemiological data indicates a prevalence of SLE in Chinese urban areas ranging from 41.77 to 53.83 per 100,000 individuals, with women being 5.27 times more likely to be affected than men.[5] The disease predominantly affects women of childbearing age. Kidney involvement occurs in about 50% of SLE patients, often progressing to lupus nephritis and potentially leading to end-stage renal disease.[6] While interventions such as glucocorticoids, hydroxychloroquine, and B-cell targeted therapies have improved

Received: 25 July 2025
Accepted: 26 September 2025
Published: 2 October 2025

patient survival rates significantly, long-term drug toxicity and disease recurrence rates remain elevated. Currently, there is still a lack of effective drug treatments for SLE. Hence, the identification of novel therapeutic targets and effective drugs holds substantial clinical importance.

Astragalus membranaceus, a traditional Chinese medicinal herb documented in the Shennong Herbal Classic, contains Astragaloside IV (AS-IV), a cycloaltane-type triterpenoid saponin recognized as a key bioactive compound.[7] AS-IV exhibits superior biological activity and efficacy compared to Astragalus polysaccharide,[8] demonstrating pharmacological properties such as anti-inflammatory, antioxidant, immunomodulatory, and anti-fibrotic effects.[9] Studies indicate that AS-IV regulates macrophage immune activity by mediating the HIF-1α/NF-κB signaling pathway. Additionally, AS-IV mitigates inflammatory responses in rats by regulating mitophagy and apoptosis. It protects against sepsis-induced acute kidney injury by alleviating mitochondrial dysfunction and apoptosis in renal tubular epithelial cells, suggesting its therapeutic potential for acute kidney injury.[10,11] Additionally, AS-IV has been observed to rebalance Th1/Th2 levels in the spleens of mice exposed to hypobaric hypoxia, reducing spleen damage and inflammation.[12] Furthermore, AS-IV attenuates renal fibrosis by modulating ALDH2-mediated autophagy to inhibit epithelial-mesenchymal transition.[13] In the context of SLE, an autoimmune condition, AS-IV exhibits anti-inflammatory and immunoregulatory effects, potentially slowing the progression of SLE. Nonetheless, the precise mechanism by which AS-IV treats SLE remains unclear, necessitating comprehensive and systematic investigations to elucidate its molecular pathways in SLE therapy, offering significant scientific and clinical value.

The core principle of network pharmacology is a research method that systematically analyzes the synergistic action mechanisms of multiple components, multiple targets, and multiple pathways of drugs based on the "disease - gene - target - drug" interaction network.[14,15] This approach is well-suited for investigating the pharmacological basis and intervention mechanisms of AS-IV compounds in treating SLE. Molecular docking, a computational chemistry technique, is utilized to predict and assess binding patterns and affinities between small molecule ligands and biomacromolecule receptors.[16] This validation of ligand-receptor interactions identified in network analysis holds significant promise for the development of novel therapeutics across diverse disease states.

In this study, we hypothesize that AS-IV can impede the progression of SLE by suppressing the immune - inflammatory response. To this end, we utilized MRL/lpr mice as lupus models, as they closely mimic the multi-organ damage observed in human SLE.[17] Through a combination of network pharmacology and in vivo assays, we examined the effectiveness, potential targets, and molecular pathways of AS-IV in treating SLE. Our findings offer novel insights into potential therapeutic approaches for SLE and establish a basis for deeper comprehension of the mechanisms underlying AS-IV's actions in autoimmune disorders.

# Materials and Methods

## Reagents and Drugs

Astragaloside IV (batch number: 2024212002) was supplied by Shanghai Yuanye Biological Co., LTD. (Shanghai, China); Prednisone (batch number: 20240318) was provided by Tianjin Tianyao Pharmaceutical Co., LTD. (Tianjin, China); ITGB1 (batch number: GR3102156-1), p-ITGB1 (batch number: GR3018265-9), p38 (batch number: GR3315660-2), IL-4 (batch number: AG19287106), IL-17 (batch number: AG18207920), IL-21 (batch number: AG19287106) AD19870462) was purchased from Santa (Shanghai, China); Kits for anti-dsDNA, IgG, C3 and C4 were provided by Wuhan Genemix Technology Co., LTD. (Wuhan, China).

## Animals and Groups

Female MRL/lpr and C57BL/6 mice (7 weeks old, 18–22 g) were obtained from Shanghai Slek Laboratory Animal Co., Ltd. (License No. SCXK2022-0004). All mice were housed under specific pathogen-free (SPF) conditions at the Animal Experiment Platform of the Hefei Comprehensive National Science Center Artificial Intelligence Research Institute. The housing environment was maintained at 25±2°C with 50±10% relative humidity, a 12-hour light/dark cycle, and provided with food and water ad libitum. All animal procedures strictly adhered to the "Regulations for the Administration of Affairs Concerning Experimental Animals of the People's Republic of China" and relevant ethical guidelines, and were

approved by the Animal Ethics Committee of Anhui University of Chinese Medicine (Approval No. AHUCM-mouse -2022130). Prepare a 10 mg/mL AS-IV solution in 5% DMSO/saline. Fifty MRL/lpr mice were randomly assigned to five groups (n=10 per group): MRL/lpr, AS-IV low-dose group (AS-IV-L, 10 mg/kg/d), AS-IV medium-dose group (AS-IV-M, 20 mg/kg/d), AS-IV high-dose group (AS-IV-H, 40 mg/kg/d), and Prednisolone group (Pred, 5 mg/kg/d). An additional group of ten C57BL/6 mice served as the control. Treatments were administered for 8 weeks. Following treatment completion, blood, spleen, and kidney samples were collected from all groups. The spleen index was calculated as spleen weight (mg) divided by body weight (g).

## Histopathology

Kidney tissues were fixed in 4% paraformaldehyde for 48h before rinsing with running water, dehydrated using ethanol, placed in xylene for transparency, embedded in paraffin, and later subjected to sectioning and deparaffinization procedures. Sections were stained with hematoxylin-eosin (HE)[18] and Masson,[19] respectively, and observed and recorded under a light microscope.

## Transmission Electron Microscope (TEM)

Ultrathin sections were prepared by primary fixation (2.5% pentylacetaldehyde), secondary fixation (1% osmium tetroxide solution), dehydration with gradient ethanol, resin infiltration, and embedding of kidney tissue. The kidneys were stained with uranyl acetate for 30 min and lead citrate for 5 min, and then rinsed thoroughly with distilled water to avoid the crystallization of stain. The structure of kidney tissue was observed and recorded by transmission electron microscope.

## T-Cell Flow Assay

The spleen tissue was cut into small pieces, filtered through a 70 μm filter, and then centrifuged with Percoll density gradient to remove dead cells and impurities to obtain purified cell suspension. Corresponding antibodies were added to 100 μL of cell solution in each group: Th1/Th2 (CD4), Treg (CD4, CD25), Th17 (CD3, CD4), and incubated for 20 min away from light. Cells were washed and resuspended in PBS, and assayed using flow cytometry. Cells were located by adjusting forward scattered light (FSC) and side scattered light (SSC), ensuring that the cells were shown on the FSC-SSC dot plot, and setting the gate to circle the target cell population, and calculating the percentage of the different T-cell subpopulations.

## Real-Time Quantitative Polymerase Chain Reaction (RT-qPCR)

The extraction of RNA was completed by grinding the kidney tissue into a powder in liquid nitrogen or collecting the cell precipitate and lysis by adding 1mL TRIzol for delamination and RNA precipitation. The RT reaction was performed to obtain cDNA. The relative mRNA expression was calculated using the $2^{-\Delta\Delta Ct}$ method. GAPDH was used as an internal control. The primers were synthesized by Anhui Zhongkang Biotechnology Co., LTD (Table 1).

## Western Blotting (WB)

Kidney tissue samples were collected, lysed by adding 600μL of RIPA cell lysate, centrifuged at 12000 r/min for 15min, and the supernatant was collected. 5X SDS-PAGE protein loading buffer was added at a ratio of 1:4 and heated in a boiling water bath for 15 min. The cooled protein samples were placed in the SDS-PAGE gel sampling Wells and

**Table 1** Primers Used for RT-qPCR

| Gene Name | Forward | Reverse |
|---|---|---|
| ITGB1 | GCCAGAAGACATTACTCAG | TCAAATCCGTTCCAAGAC |
| PTK2 | ACTTGGACGCTGTATTGGAG | CTGTTGCCTGCTTTCTGGAT |
| p38 | CTCATTAACAGGATGCCAAGC | CTTGGGCCGCTGTAATTCTC |
| GAPDH | TTCCACCCATGGCAAATTCC | ATCTCGCTCCTGGAAGATGG |

subjected to constant pressure of 80V for protein electrophoresis for 1h. The proteins were transferred to PVDF membrane after 1 h of membrane transfer and blocked for 2 h at room temperature on a shaker. After incubation with primary antibodies, ITGB1 (1:2000), p-ITGB1 (1:10,000), PTK2 (1:1500), p38 (1:2000) and GAPDH (1:2000) were added, and HRP-labeled secondary antibodies (Goat Anti-Mouse IgG, 1:20000) were added and incubated at room temperature for 1.2 hours. The ECL luminescence kit was used to take pictures with the chemiluminescence imaging system, and Image J software was used for gray level analysis.

## Biochemical Kit Testing

Mouse urine was collected, and 24-hour urine protein quantification (24hPRO), total protein, albumin, and creatinine were detected using a urine protein quantification kit, urine protein kit, and urine creatinine kit, respectively. The urine total protein-to-creatinine ratio (UTPCR) was calculated.

## Enzyme-Linked Immunosorbent Assay (ELISA)

The whole blood of mice was collected and centrifuged to obtain serum. ELISA kits were used to detect the levels of anti-dsDNA, immunoglobulin G (IgG), complement 3 (C3) and complement 4 (C4) in serum. The specific operation procedure was referred to the kit instruction manual.[20]

## Immunofluorescence Staining

Kidney tissue sections were deparaffinized in xylene, followed by antigen repair, addition of 0.3% Triton X-100, permeabilization and blocking at room temperature. Primary antibodies: GATA3 (1:200), Foxp3 (1:200), ITGB1 (1:300), IL-21 (1:500) were added, and the cells were incubated at 37°C for 60 min. Secondary antibody was added by dropping: proper amount of HRP-labeled secondary antibody reagent was added and incubated at room temperature in the dark for 30 min. TSA fluorescent dye was added dropfold, the cells were incubated at room temperature in the dark for 10 min, and washed three times with PBS. The sections were counterstained by dropping an appropriate amount of DAPI staining solution. The tablets were sealed with anti-fluorescence quenching sealant, and the images were observed under a fluorescence microscope and collected.

## Immunohistochemical Staining

The renal tissue sections were incubated in 3% $H_2O_2$ at room temperature for 10 min and washed with PBS for 3 times. 5% BSA was added dropingly and sealed at room temperature for 30 min. Primary antibodies: RORγt (1:200), PTK2 (1:200), IL-4 (1:100), and IL-17 (1:100) were added drop by drop and incubated at 37 °C for 60 min. Secondary antibody was added dropatively: an appropriate amount of HRP-labeled secondary antibody reagent was added and incubated at 37 °C for 30 min. The slides were counterstained with hematoxylin for 2 min, blued with lithium carbonate solution for 30s, sealed with neutral gum, and observed under a microscope.

## Network Pharmacology

The chemical structure and canonical SMILES representation were first retrieved by searching for the keyword "Astragaloside IV" in the PubChem database[21] (Accessed on 18 March 2025, https://pubchem.ncbi.nlm.nih.gov/). The target genes were collected using ChEMBL database[22] (Accessed on 18 March 2025, https://www.ebi.ac.uk/chembl/) and SwissTargetPrediction database[23] (Accessed on 19 March 2025, http://swisstargetprediction.ch/). The UniProt database was also used to normalize the protein names to obtain the final Astragaloside IV gene set. Next, from the GeneCards database[24] (Accessed on 19 March 2025, https://www.genecards.org/), the OMIM database[25] (Accessed on 19 March 2025, https://omim.org/), the TTD database[26] (Accessed on 19 March 2025, https://db.idrblab.net/ttd/), and the Disgenet database[27] (Accessed on 19 March 2025, https://disgenet.com/) to collect SLE target genes, and the SLE gene set was obtained by combining the genes obtained from the four databases and removing duplicates. The above two sets were used to obtain the intersecting genes using Venn diagrams, and the common targets were imported into the STRING database (Accessed on 21 March 2025, https://cn.string-db.org/) for protein-protein interaction (PPI) analysis to screen the core targets, which were visualized and analyzed in Cytoscape software (3.10.2). Finally, gene ontology (GO)

analysis and Kyoto Encyclopedia of Genes and Genomes (KEGG) pathway enrichment analysis were performed using the Metascape database[28] (http://metascape.org).

## Molecular Docking

The molecular structures of the core targets, namely ITGB1, PTK2, and p38, were retrieved from the Protein Data Bank (PDB) database[29] (Accessed on 22 March 2025, https://www.rcsb.org/). The PDB IDs for ITGB1, PTK2, and p38 are 1JV2, 2J0J, and 3PY3, respectively. Meanwhile, the three-dimensional structure of Astragaloside IV was obtained from the PubChem database. Subsequently, molecular docking was carried out using AutoDock Vina software (v1.5.7, The Scripps Research Institute) to identify potential binding sites. To gain a more intuitive understanding of the docking outcomes, the results were visualized with the help of PyMOL software (v2.5.4, DeLano Scientific LLC). This visualization step was crucial for comprehensively assessing the binding affinity between the ligand (AS-IV) and the receptors (ITGB1, PTK2, and p38).

## Statistical Analysis

Each experiment was independently repeated at least five times. GraphPad Prism v9.5.1 (GraphPad Software) and SPSS Statistics v27.0 (IBM Corp.) were applied for statistical analysis and data visualization. The measurement data were expressed as mean ± standard deviation, and two independent samples *t*-test was used for comparisons between groups that conformed to normal distribution, and non-parametric tests were used for those that did not conform to normal distribution. A p-value of less than 0.05 indicated a statistically significant difference.

# Results

## AS-IV Ameliorates Renal Histopathologic Damage in MRL/Lpr Mice

To assess the impact of AS-IV on renal tissues, kidney specimens from all experimental groups were processed for HE staining and Masson's trichrome staining. HE staining results revealed that the MRL/lpr group exhibited prominent intracapillary and mesangial cell proliferation, thickening of the glomerular basement membrane, and extensive lymphocyte infiltration. In contrast, in the AS-IV-L, AS-IV-M, AS-IV-H, and Pred groups, both cell proliferation and mesangial thickening were mitigated, and lymphocyte infiltration was notably reduced compared to the MRL/lpr group (Figure 1A). Masson's trichrome staining demonstrated that the MRL/lpr group displayed marked fibrotic changes in the glomerular capillary lumens, substantial basement membrane thickening, and partial global glomerulosclerosis. Conversely, fibrotic lesions were significantly attenuated in the AS-IV-L, AS-IV-M, AS-IV-H, and Pred groups. Among them, the Pred group showed the least severe fibrosis (Figure 1B). Compared withdamage (Figure 1C and D, $P < 0.01$). The AS-IV-L, AS-IV-M, and AS-IV-H groups showed significant reductions in these scores compared to the MRL/lpr group ($P < 0.01$, $P < 0.05$). Biochemical kits were used to measure 24hPRO and UTPCR in each group. Compared with the control group, the MRL/lpr group exhibited significantly elevated 24hPRO and UTPCR levels (Figure 1E and F, $P < 0.01$). After AS-IV treatment, both parameters decreased to levels comparable to those of the Pred group, with no statistically significant difference observed between the two treatment groups. Collectively, these findings suggest that AS-IV is as effective as Pred in ameliorating renal histopathological damage.

## Effect of AS-IV on Kidney Ultrastructure in MRL/Lpr Mice

Transmission electron microscopy (TEM) findings provided detailed insights into the renal ultrastructure. In the Control group, glomerular mesangial cells exhibited a characteristic star-shaped morphology, featuring multiple protrusions of unequal lengths. The distinct structures of dense plaques and dense bodies were clearly discernible. In contrast, the MRL/lpr group presented a marked pathological phenotype. Electron-dense deposits were prominently observed in the glomerular mesangial area, accompanied by evident mesangial cell proliferation and an increase in the extracellular matrix. However, in the AS-IV-L, AS-IV-M, AS-IV-H, and Pred groups, there was a notable alleviation of these pathological features. Specifically, the deposition of electron-dense materials in the glomerular mesangial area and the degree of mesangial cell proliferation were significantly reduced compared to the MRL/lpr group (Figure 2A–F). Quantitative analysis further

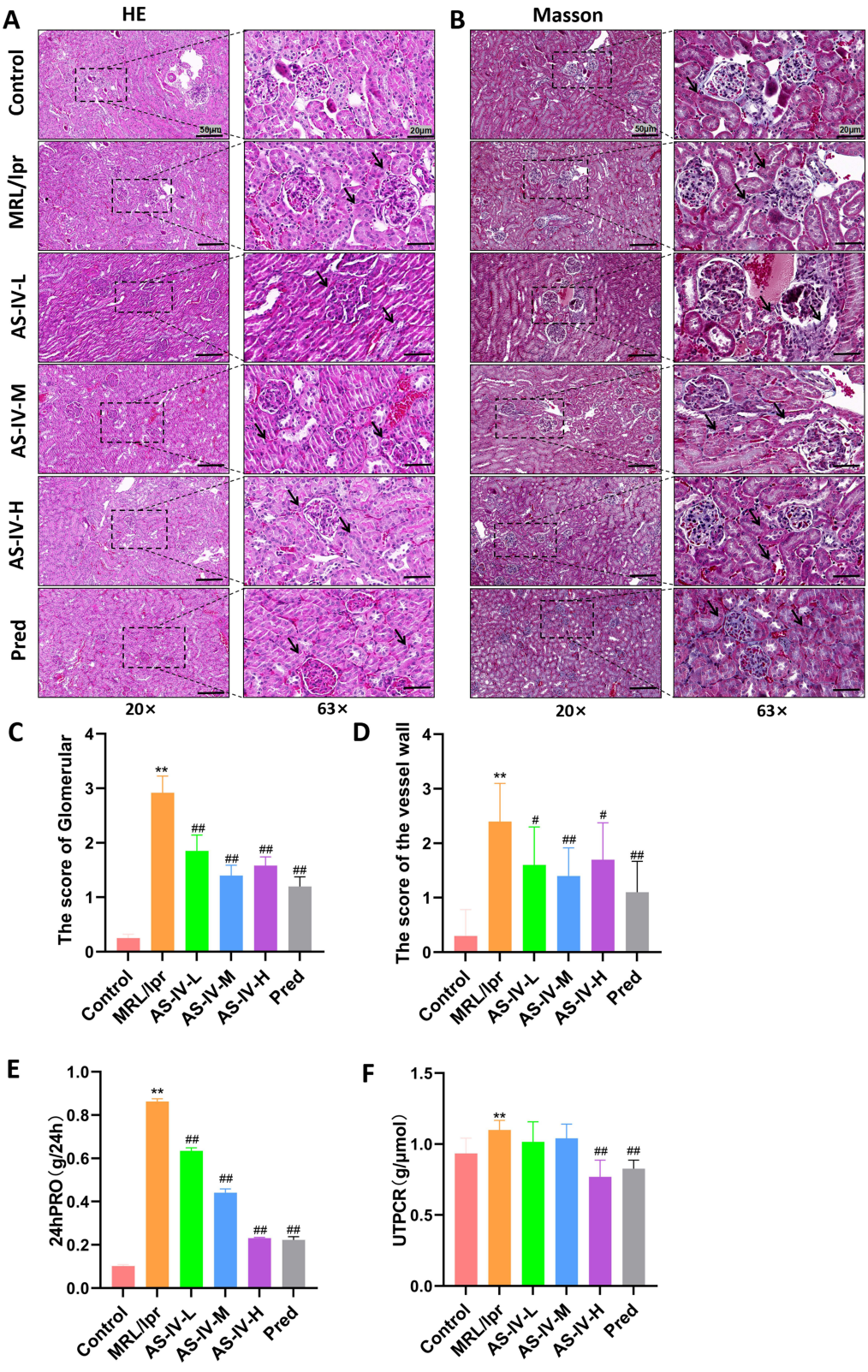


**Figure 1** AS-IV ameliorated renal histopathological damage in MRL/lpr mice. (**A**) HE staining of kidney tissue. (**B**) Masson staining of kidney tissue. (**C**) Glomerular scores of mice in each group. (**D**) Renal vessel wall scores of mice in each group. (**E**) 24-hour urine protein (24hPRO) quantification in each group. (**F**) Urine total protein-to-creatinine ratio (UTPCR) in each group. Data are presented as mean ± SD (n=10). $^{**}P < 0.01$ compared with the Control group; $^{\#\#}P < 0.01$, $^{\#}P < 0.05$ compared with the MRL/lpr group. Each experiment was repeated ten times.

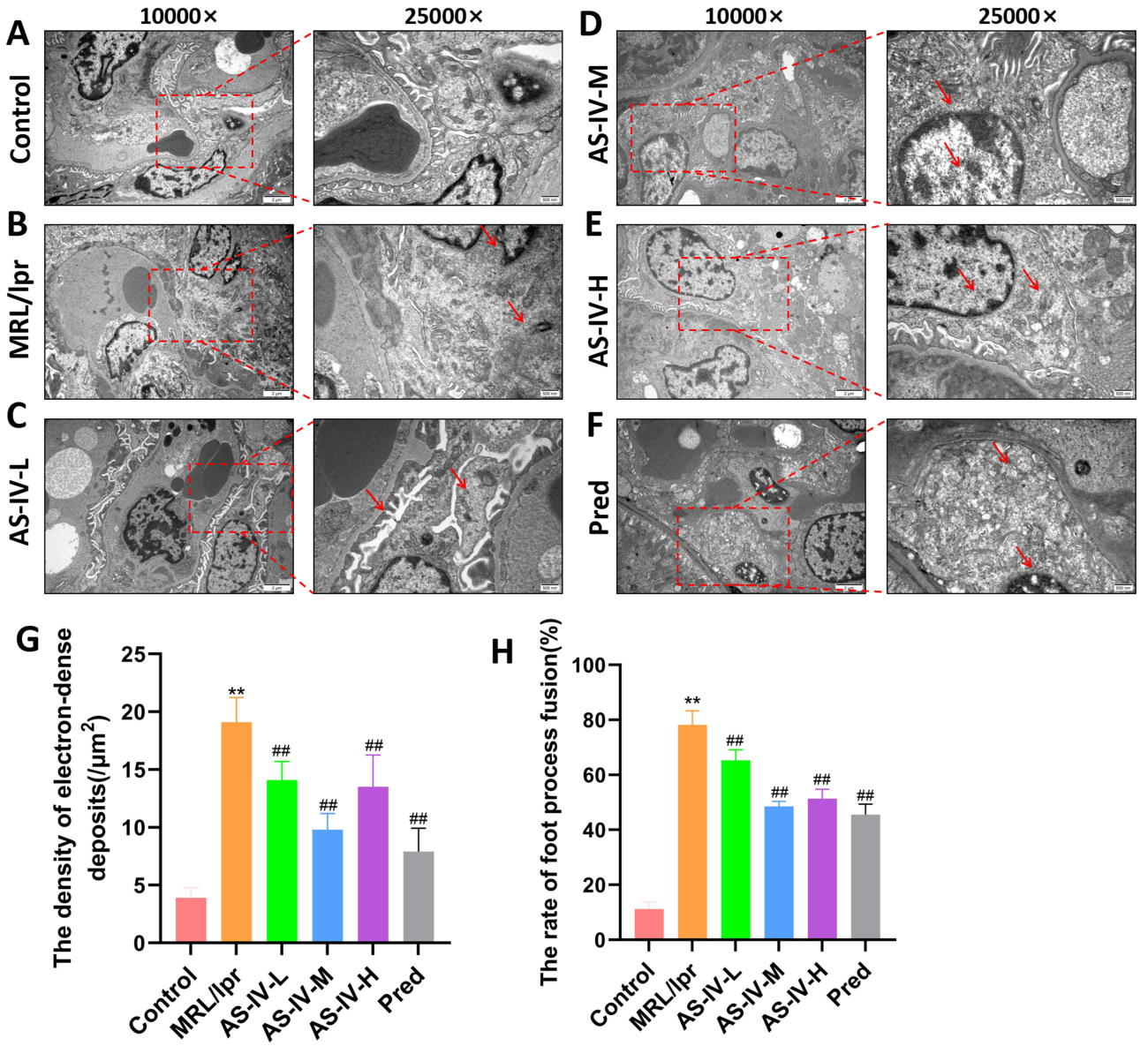


**Figure 2** Transmission electron microscopy (TEM) observation of the ultrastructure of the kidneys in MRL/lpr mice. (**A**–**F**) TEM images of the kidneys of mice in each group. (**G**) Density of electron-dense deposits in mice of each group. (**H**) Foot-process effacement rate in mice of each group. Data are presented as mean ± SD (n=10). $^{**}P < 0.01$ compared with the Control group; $^{\#\#}P < 0.01$ compared with the MRL/lpr group. Each experiment was repeated ten times.

demonstrated that AS-IV effectively decreased the density of electron-dense deposits and the foot process fusion rate in the kidneys of MRL/lpr mice (Figure 2G and H, $P < 0.01$). Collectively, these results strongly suggest that AS-IV can mitigate the deposition of immune complexes, thereby alleviating the severity of renal damage.

## AS-IV Improves Immune Function in MRL/Lpr Mice

The intervention effect of AS-IV was evaluated by calculating the spleen index of each group and detecting immune function-related indicators using ELISA. The results showed that compared with the Control group, the spleen index in the MRL/lpr group was significantly increased ($P < 0.01$). After intervention with AS-IV or Pred, the spleen index was significantly decreased (Figure 3A and B, $P < 0.01$). Compared with the MRL/lpr group, the levels of IgG and anti-dsDNA in the AS-IV-L, AS-IV-M, AS-IV-H, and Pred groups were significantly decreased (Figure 3C and D, $P < 0.01$), while the levels of C3 and C3 were significantly increased (Figure 3E and F, $P < 0.01$). These results revealed that AS-IV has the effect of improving the immune function of MRL/lpr mice.


https://doi.org/10.2147/DDDT.S554510

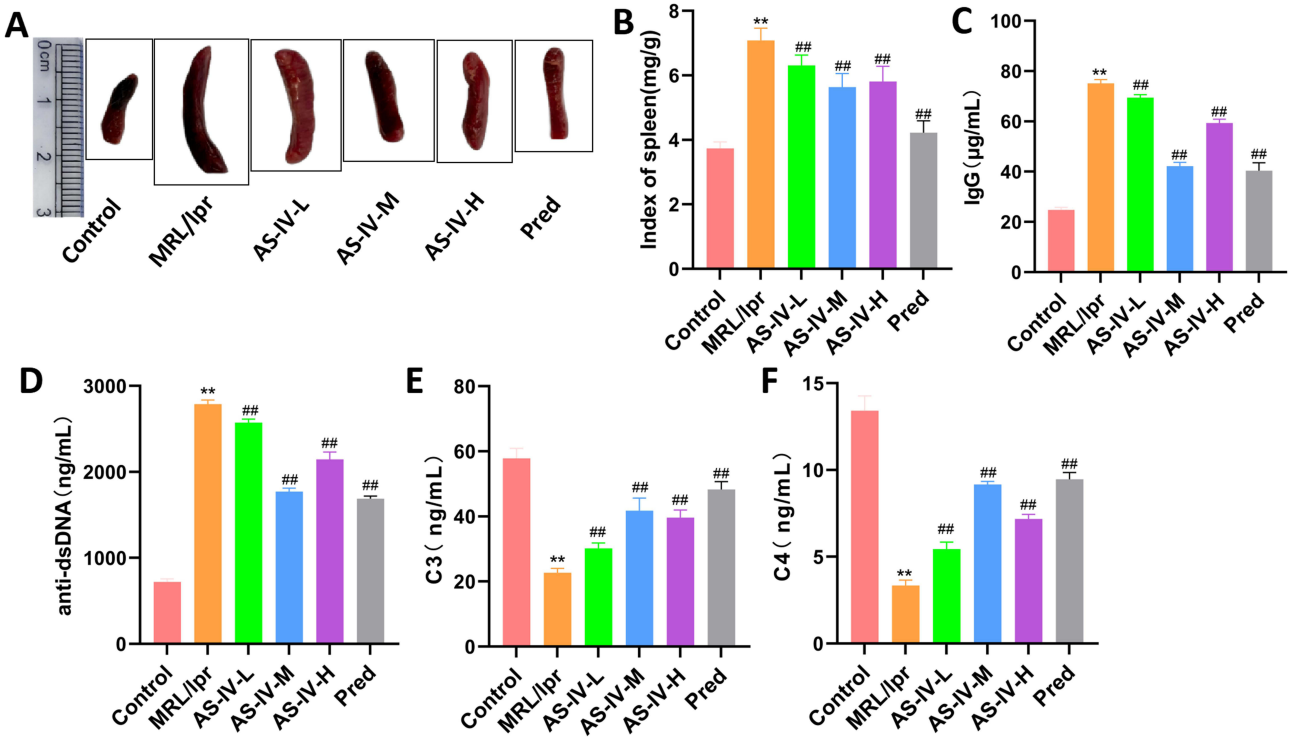


**Figure 3** AS-IV improves the immune function of MRL/lpr mice. (**A** and **B**) Spleen indices of mice in each group. (**C**–**F**) Levels of IgG, anti-dsDNA, C3, and C4 in mice of each group detected by ELISA. Data are presented as mean ± SD (n=10). $^{**}P < 0.01$ compared with the Control group; $^{\#\#}P < 0.01$ compared with the MRL/lpr group. Each experiment was repeated ten times.

## AS-IV Improves T-Cell Subset Ratio in MRL/Lpr Mice

The proportion of T cell subsets in each group of mice was detected by flow cytometry (Figure 4A). The results showed that compared with the Control group, the ratio of Th1/Th2 and the proportion of Th17 cells in the MRL/lpr group were increased ($P < 0.01$), while the proportion of Treg cells was decreased ($P < 0.01$). After the intervention of AS-IV, the ratio of Th1/Th2 and the proportion of Th17 cells in MRL/lpr mice were significantly decreased ($P < 0.01$), and the proportion of Treg cells was significantly increased ($P < 0.01$). The intervention effect of Astragaloside IV was comparable to that of Pred (Figure 4B–D). These results indicate that Astragaloside IV can improve the proportion of T cell subsets in MRL/lpr mice.

## Effect of AS-IV on T-Cell Differentiation-Related Factors in MRL/Lpr Mice

Immunohistochemistry and immunofluorescence staining were employed to detect the expression of T-cell differentiation-related factors in each experimental group (Figure 5A). The results revealed that, in comparison with the Control group, the MRL/lpr group exhibited a significant decrease in Foxp3 expression and an increase in the expression of GATA3, RORγt, and T-bet ($P < 0.01$). In MRL/lpr mice, AS-IV significantly upregulated Foxp3 expression and downregulated the expression of GATA3, RORγt, and T-bet (Figure 5B–E, $P < 0.01$, $P < 0.05$). Among the treatment groups, the AS-IV-M group demonstrated the most pronounced intervention effect, comparable to that of the Pred group. Collectively, these findings suggest that Astragaloside IV can modulate T-cell differentiation in MRL/lpr mice.

## Network Pharmacology Analysis of Potential Targets of AS-IV in SLE

We retrieved 94 target genes associated with AS-IV and 2444 target genes related to SLE from multiple authoritative databases. Subsequently, 34 intersection genes were identified (Figure 6A and B). Using PPI network analysis, we pinpointed nine core targets, namely ITGB1, PTK2, MAPK14, CXCL8, and LGALS3 (Figure 6C–E). KEGG and GO

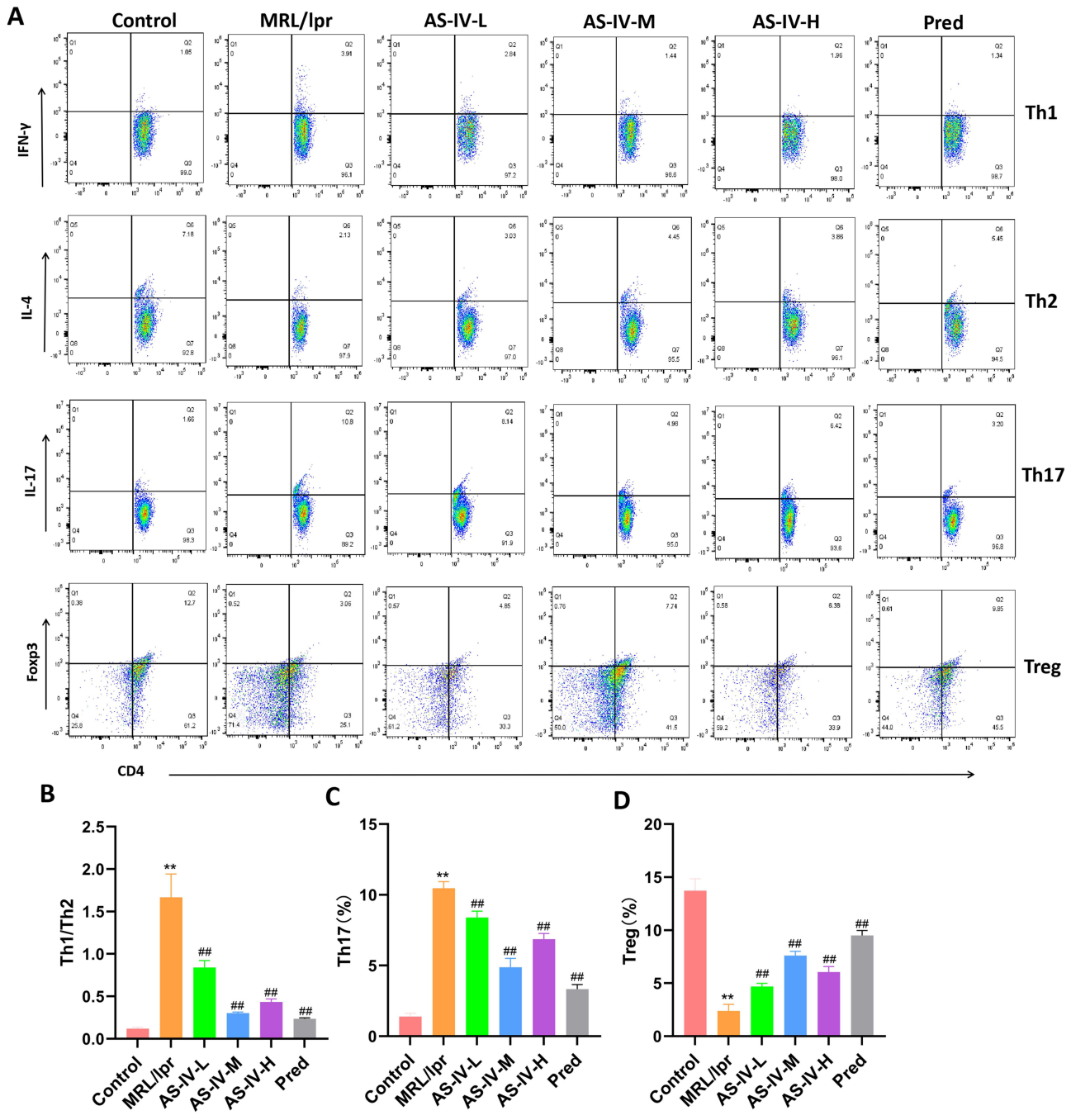


**Figure 4** AS-IV improves the proportion of T cell subsets in MRL/lpr mice. (**A**) The proportion of Th1, Th2, Th17 and Treg cells in each group was detected by flow cytometry. (**B**) Th1/Th2 ratio of mice in each group. (**C** and **D**) The proportion of Th17 and Treg cells in each group. Data are presented as mean ± SD (n=10). $^{**}P < 0.01$ compared with the Control group; $^{\#\#}P < 0.01$ compared with the MRL/lpr group. Each experiment was repeated ten times.

enrichment analyses of the 34 intersection genes indicated that the underlying mechanism of AS-IV's action is linked to cell differentiation, integrin binding, the extracellular matrix, and the ITGB1/PTK2/p38 signaling axis (Figure 6F and G).

## Effects of AS-IV on the ITGB1/PTK2/p38 Signaling Axis in MRL/Lpr Mice

To comprehensively explore the regulatory effects of AS-IV on the ITGB1/PTK2/p38 signaling axis, we employed multiple experimental techniques, including Western blotting, RT-qPCR, immunofluorescence, and immunohistochemistry. The expression levels of ITGB1, PTK2, and p38 in the MRL/lpr group were significantly elevated compared to


https://doi.org/10.2147/DDDT.S554510

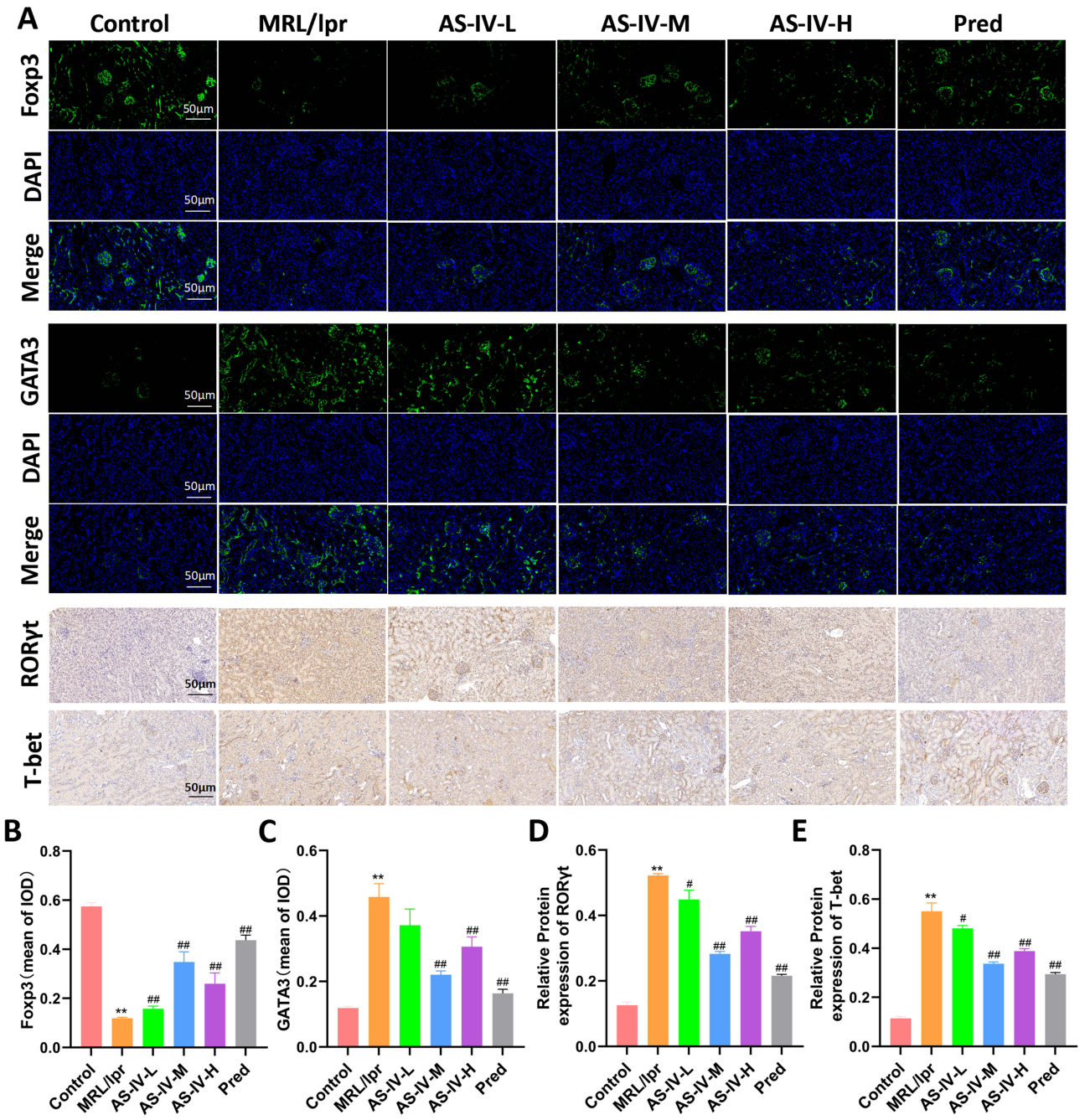


**Figure 5** Effect of AS-IV on factors associated with T-cell differentiation in MRL/lpr mice. (**A**) Immunofluorescence and immunohistochemical staining were used to detect the expression of Foxp3, GATA3, RORγt and T-bet. (**B** and **C**) Mean optical density of Foxp3 and GATA3 in each group. (**D** and **E**) Expression levels of RORγt and T-bet in each group. Data are presented as mean ± SD (n=10). $^{**}P < 0.01$ compared with the Control group; $^{\#\#}P < 0.01$, $^{\#}P < 0.05$ compared with the MRL/lpr group. Each experiment was repeated ten times.

those in the Control group ($P < 0.01$). This indicates a dysregulation of the ITGB1/PTK2/p38 signaling pathway in the MRL/lpr mice model. Immunofluorescence and Western blotting results demonstrated that AS-IV effectively decreased the protein levels of p-ITGB1, PTK2, and p38 in MRL/lpr mice (Figure 7A–E, $P < 0.01$). This suggests that AS-IV can directly modulate the protein abundance within the signaling axis. Immunohistochemistry and RT-qPCR analyses showed that AS-IV also led to a significant reduction in the mRNA expression of ITGB1, PTK2, and p38 (Figure 7F–J, $P < 0.01$). These findings imply that AS-IV may act at the transcriptional level to regulate the signaling pathway. To further validate the potential targets of AS-IV, molecular docking technology was utilized to assess its binding affinity to ITGB1, PTK2,

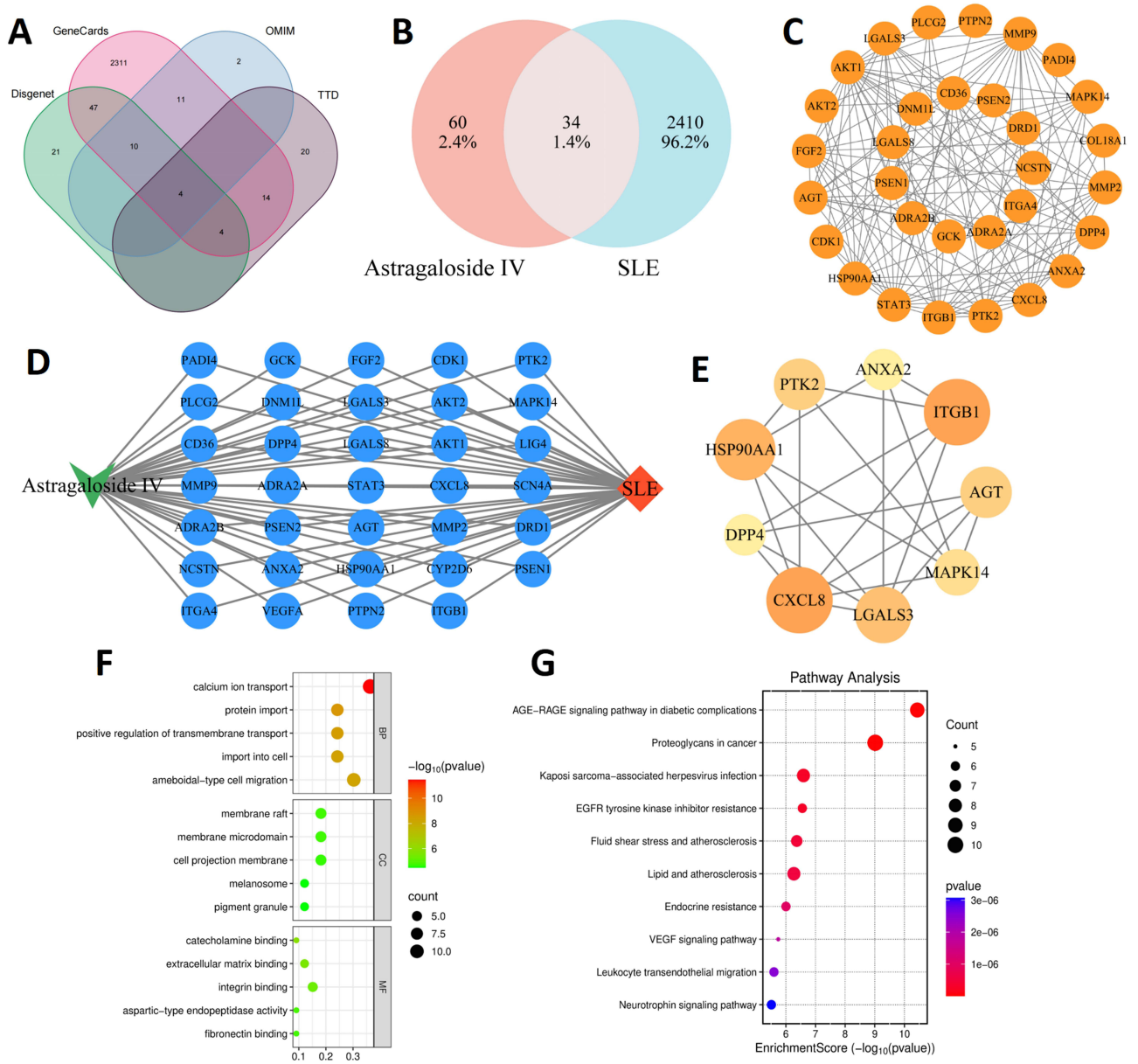


**Figure 6** Network pharmacology analysis of potential targets of AS-IV in SLE. (**A** and **B**) AS-IV targets were intersected with SLE targets. (**C**) Construct PPI network. (**D**) Drug-disease-target network diagram. (**E**) Screening of core targets. (**F** and **G**) GO and KEGG analysis results.

and p38. The results revealed that the minimum binding energies of AS-IV with ITGB1, PTK2, and p38 were −8.2 kcal/mol, −6.4 kcal/mol, and −7.9 kcal/mol, respectively (Figure 8). These negative binding energies suggest a strong binding ability of AS-IV to these key molecules of the signaling axis. Collectively, these results strongly suggest that AS-IV exerts its regulatory effects by acting on the ITGB1/PTK2/p38 signaling axis, providing a potential molecular mechanism for its therapeutic application in relevant diseases.

## Effect of AS-IV on Renal Cytokines in MRL/Lpr Mice

Immunohistochemical and immunofluorescent staining were employed to assess the expression of renal cytokines. Key findings were as follows: In the MRL/lpr group, the expression levels of IL-4, IL-17, and IL-21 were significantly elevated compared to the Control group ($P < 0.01$). In the AS-IV-L, AS-IV-M, AS-IV-H, and Pred groups, there was a significant reduction in the expression of IL-4, IL-17, and IL-21 when compared to the MRL/lpr group (Figure 9A–E,


https://doi.org/10.2147/DDDT.S554510

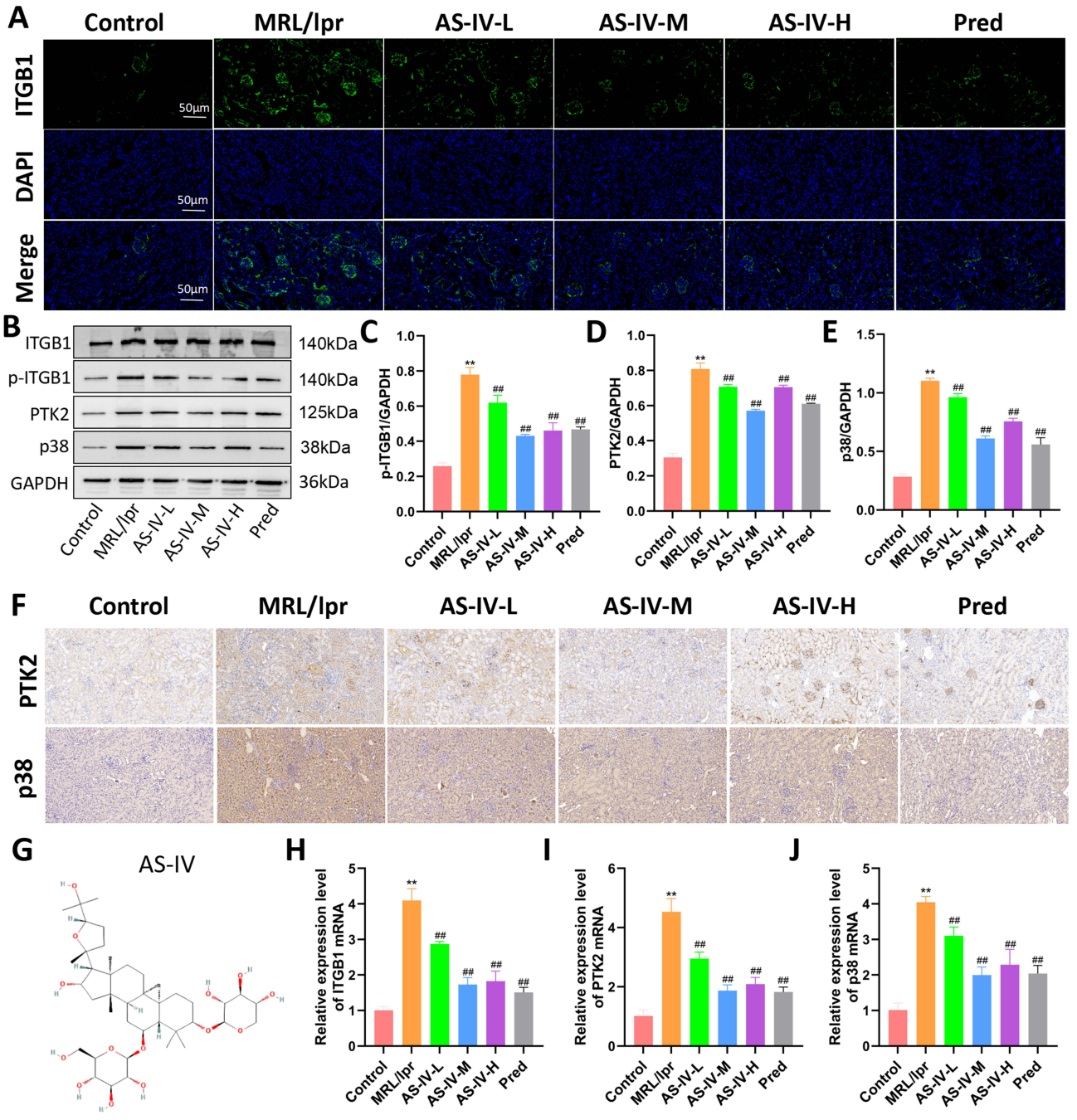


**Figure 7** Effect of AS-IV on ITGB1/PTK2/p38 signaling axis in MRL/lpr mice. (**A**) Immunofluorescence staining to detect the expression of ITGB1 in each group of mice. (**B**–**E**) Protein blotting to detect the expression of p-ITGB1, PTK2, and p38 proteins in each group of mice. (**F**) Immunohistochemical staining to detect the expression of PTK2 and p38 in each group of mice. (**G**) Molecular formula of AS-IV. (**H**–**J**) RT-qPCR to detect the expression of ITGB1, PTK2 and p38 mRNA. Data are presented as mean ± SD (n=10). $^{**}P < 0.01$ compared with the Control group; $^{\#\#}P < 0.01$ compared with the MRL/lpr group. Each experiment was repeated ten times.

$P < 0.01$ or $P < 0.05$). Among them, the AS-IV-M group exhibited the most pronounced intervention effect, comparable to that of the Pred group. These results strongly suggest that AS-IV effectively downregulates cytokine expression, thereby alleviating the inflammatory response in the kidneys of MRL/lpr mice.

## Discussion

Systemic lupus erythematosus (SLE) represents a multifactorial autoimmune disorder characterized by dysregulated immune cell function, pathological immune complex deposition, and aberrant overproduction of inflammatory mediators,

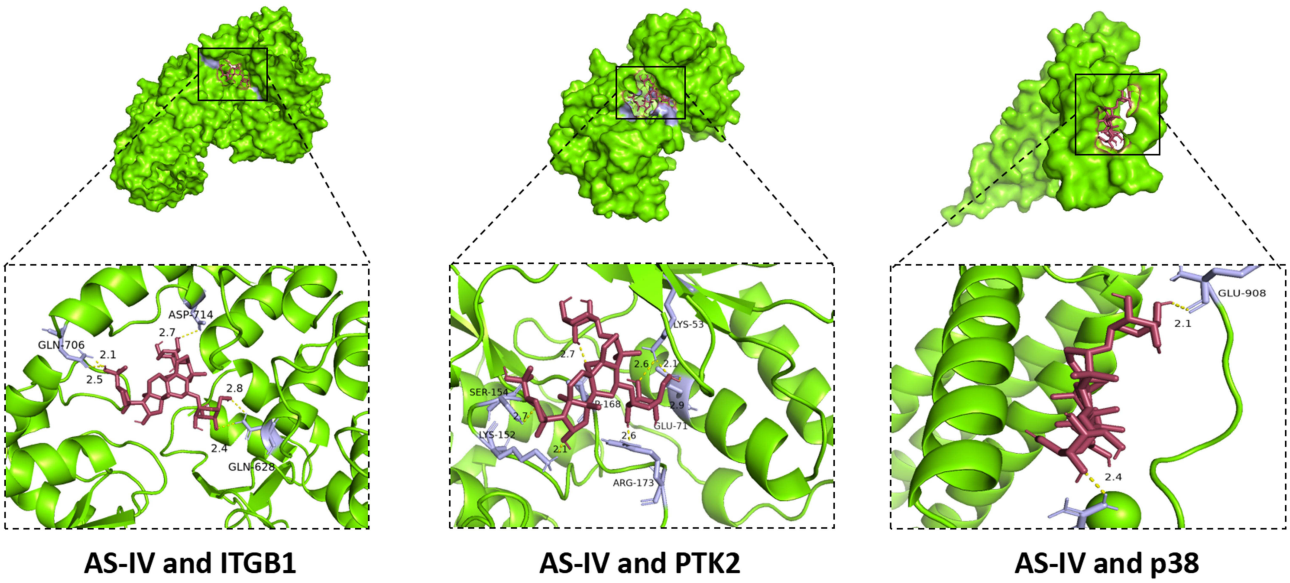


**Figure 8** Molecular docking results of AS-IV with ITGB1, PTK2, and p38.

culminating in multi-organ damage.[1] Current clinical management of SLE primarily relies on conventional therapeutics including glucocorticoids and immunosuppressive agents. While effective for disease control, chronic administration of these pharmacotherapies induces significant adverse effects, including heightened infection risk, osteoporosis, and metabolic derangements.[30,31] Consequently, the development of novel therapeutic agents remains an imperative research focus. Astragalus membranaceus (Huangqi), a traditional immunomodulatory botanical medicine with extensive clinical history, demonstrates established efficacy in immune regulation.[32] Preliminary investigations identified astragaloside IV (AS-IV), a bioactive saponin isolated from Astragalus membranaceus, as a compound of significant pharmacological interest.[33] This study comprehensively evaluated the therapeutic efficacy of AS-IV in the MRL/lpr murine lupus model. Employing an integrated approach combining network pharmacology and molecular docking, we elucidated its underlying mechanisms. Key findings demonstrate that AS-IV: Significantly ameliorates renal pathology, Attenuates glomerular immune complex deposition, Suppresses systemic and renal inflammation. Notably, the therapeutic potency of AS-IV proved comparable to glucocorticoid treatment. Collectively, these data validate the therapeutic potential of AS-IV for SLE intervention and provide mechanistic insights supporting its clinical translation.

In this study, MRL/lpr mice were administered AS-IV for eight weeks. Our findings revealed that AS-IV exerted a notable protective effect on the kidneys. Histopathological analysis via HE and Masson staining indicated that AS-IV significantly mitigated glomerular mesangial proliferation, lymphocyte infiltration, and renal fibrosis. Renal histopathology serves as a reliable indicator of the extent of kidney damage.[34] To gain deeper insights into the ultrastructural alterations in the kidneys, transmission electron microscopy was employed. The results demonstrated that AS-IV effectively alleviated immune complex deposition and foot-process effacement in the kidneys of MRL/lpr mice, with its efficacy comparable to that of prednisone. SLE is clinically characterized by the presence of anti-double-stranded DNA (anti-dsDNA) antibodies, elevated immunoglobulin levels, and complement depletion.[35] Anti-dsDNA antibodies are a quintessential biomarker of SLE, and fluctuations in their levels have a profound impact on the diagnosis, treatment, and prognosis of the disease.[36] It has been established that anti-dsDNA antibodies can trigger thrombosis by directly activating platelets.[37] In the pathogenesis of SLE, TRIM21 has been identified as a novel modulator of the cGAS-STING signaling pathway. TRIM21 can influence type I interferon production and promote the generation of anti-dsDNA antibodies by inhibiting the autophagic degradation of STING through p62/SQSTM1 ubiquitination.[38] Our experimental results showed that AS-IV effectively decreased the spleen index, anti-dsDNA antibody levels, and immunoglobulin G levels, while increasing complement levels. These findings strongly suggest that AS-IV can restore the immune homeostasis in MRL/lpr mice.


https://doi.org/10.2147/DDDT.S554510

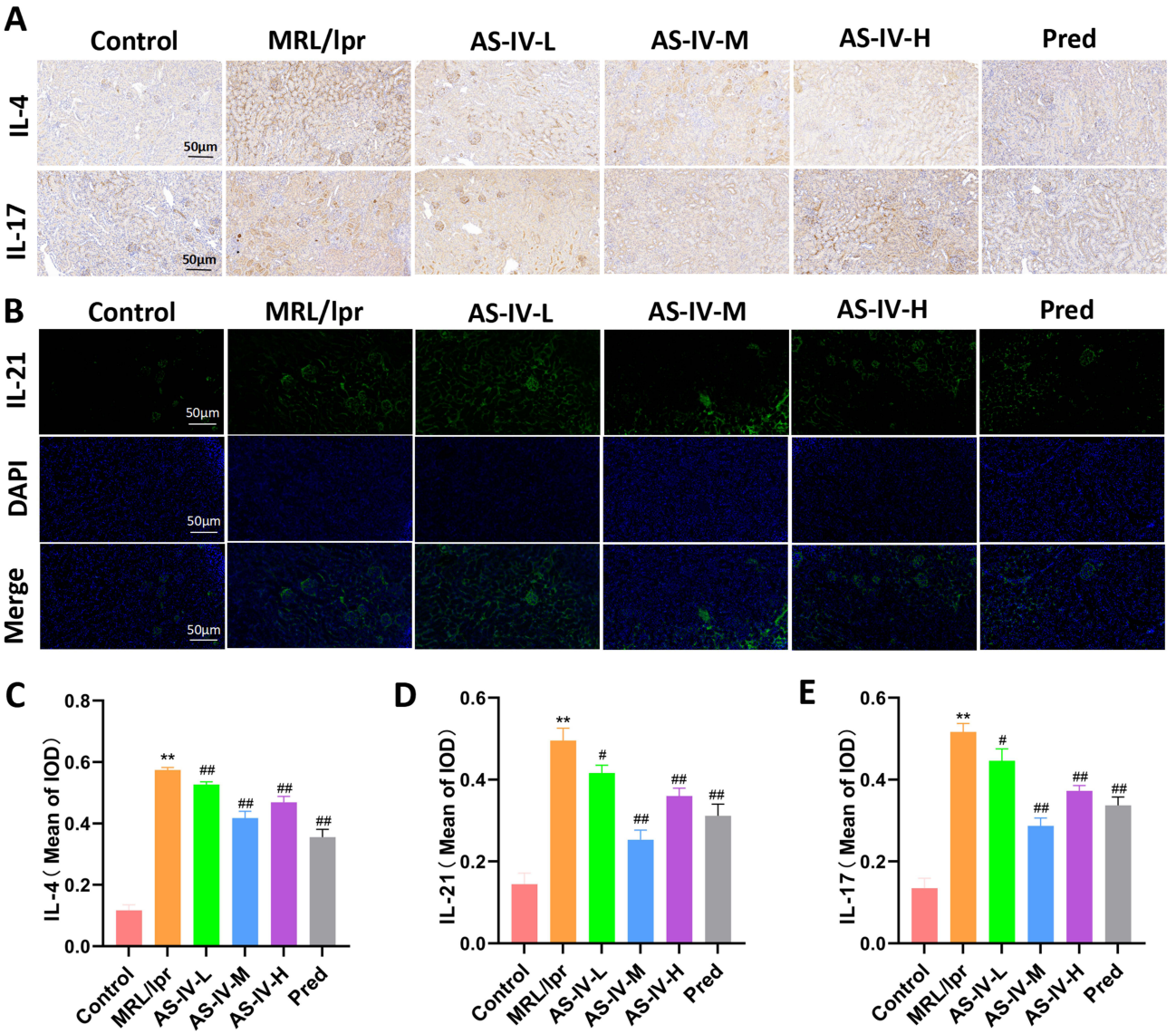


**Figure 9** Effect of AS-IV on renal cytokines in MRL/lpr mice. (**A** and **B**) Immunohistochemical staining and immunofluorescence staining were used to detect the expression of IL-4, IL-17 and IL-21. (**C**–**E**) Mean optical density values of IL-4, IL-17 and IL-21 in each group. Data are presented as mean ± SD (n=10). $^{**}P < 0.01$ compared with the Control group; $^{\#\#}P < 0.01$, $^{\#}P < 0.05$ compared with the MRL/lpr group. Each experiment was repeated ten times.

SLE is characterized by profound immune dysregulation, primarily manifesting as an imbalance in T-cell subsets and excessive activation of B cells. In this study, we employed a comprehensive multi-omics approach, including ELISA, flow cytometry, immunofluorescence, and immunohistochemistry, to evaluate the immunomodulatory effects of AS-IV. Our findings demonstrated that AS-IV significantly normalized the Th1/Th2 and Th17 cell ratios while up-regulating the proportion of Treg cells. Concomitantly, AS-IV effectively reduced the expression of key pro-inflammatory cytokines, namely IL-4, IL-21, and IL-17. IL-4, a signature cytokine secreted by Th2 cells, is intricately involved in the humoral immune response.[39] Elevated IL-4 levels are commonly observed in SLE patients, and previous research has indicated that blocking IL-4 signaling may hold therapeutic potential for SLE.[40] IL-21, secreted by Th17 and T follicular helper (Tfh) cells, is a crucial mediator that promotes B-cell activation and antibody production, thereby playing a pivotal role in the pathogenesis of SLE.[41,42] IL-17, a hallmark cytokine of Th17 cells, is central to the inflammatory cascade in autoimmune diseases.[43] Correlative studies have established a positive association between serum IL-17 levels and SLE disease activity, as well as renal and nervous system involvement.[44] The inhibitory effect of AS-IV on these pro-inflammatory cytokines is likely to contribute to the restoration of immune homeostasis and the mitigation of

inflammatory damage. Moreover, the ability of AS-IV to regulate the Th1/Th2 and Th17 cell ratios and enhance the proportion of Treg cells further underscores its potential as an immunomodulatory agent in the context of SLE.[45] To explore the mechanism by which AS-IV modulates T-cell subsets, we further investigated the expression of T-cell differentiation-related factors. The results indicated that AS-IV significantly upregulated the expression of Foxp3, a key transcription factor specific to Treg cells, while downregulating the expression of GATA3, RORγt, and T-bet. GATA3 is associated with Th2 cell differentiation, RORγt is crucial for Th17 cell differentiation, and T-bet is a master regulator of Th1 cell differentiation. These findings are consistent with the previous observations on the effects of AS-IV on T-cell subset ratios. Mechanistically, AS-IV exerts its immunomodulatory and anti-inflammatory effects by precisely regulating the balance of T-cell subsets. By promoting Treg cell function and inhibiting the differentiation of pro-inflammatory Th1, Th2, and Th17 cells, AS-IV restores the disrupted immune equilibrium in SLE. This suggests that AS-IV holds significant potential as a therapeutic agent for the treatment of SLE, offering a novel approach to address the complex immunopathology of this disease.

Our prior research substantiated the efficacy of AS-IV in treating SLE. Subsequently, we employed network pharmacology to identify the potential molecular targets of AS-IV. The analysis revealed core targets including ITGB1, PTK2, MAPK14, and CXCL8. ITGB1, a transmembrane protein, participates in cell-extracellular matrix interactions, cell-cell adhesion, migration, and signal transduction.[46] In SLE patients, aberrant ITGB1 expression can trigger abnormal activation and migration of immune cells, facilitating immune complex deposition and the onset of inflammatory responses.[47] PTK2, also referred to as focal adhesion kinase (FAK), serves as a crucial downstream signaling molecule of ITGB1. It mediates cell adhesion signaling through autophosphorylation at tyrosine residue 397 (Y397).[48] A previous study reported that the interaction between ITGB1 and T cells in SLE induces FAK-mediated signaling,[49] which enhances the activation of autoreactive T cells, aligning with our network pharmacology findings. MAPK14, known as p38 mitogen-activated protein kinase, is pivotal in the inflammatory response, promoting the synthesis of inflammatory factors.[50] CXCL8, a chemotactic factor, attracts immune cells such as neutrophils to the inflammatory site, thereby exacerbating the inflammatory process.[51] These targets are intricately interconnected, forming a complex signaling network that collectively contributes to the pathogenesis of SLE. This network provides a mechanistic basis for understanding how AS-IV exerts its therapeutic effects in SLE treatment.

In our pursuit to further validate the impact of AS-IV on the potential targets ITGB1, PTK2, and p38, we employed an MRL/lpr mouse model, a well-established animal model for SLE. In MRL/lpr mice, we observed upregulated expression of ITGB1, PTK2, and p38, which is consistent with the pathological features of SLE. However, treatment with AS-IV effectively downregulated the expression levels of these proteins. This finding strongly suggests that AS-IV can act on these potential targets, interrupt the activation of associated signaling pathways, and thus exert its therapeutic efficacy. From a signal transduction perspective, upon binding to its ligand, ITGB1 initiates the activation of PTK2. Subsequently, activated PTK2 triggers the downstream p38 mitogen-activated protein kinase (MAPK) signaling pathway.[52,53] This cascade ultimately leads to the production of inflammatory factors and the activation of immune cells, as previously reported in the literature. By suppressing the expression of ITGB1, PTK2, and p38, AS-IV can disrupt this signaling axis, curtail the release of inflammatory factors, and modulate the function of immune cells.Molecular docking technology offered us direct insights into the interaction between AS-IV and these potential targets. Through molecular docking analysis, we discovered that AS-IV can form a stable binding conformation with the target sites of ITGB1, PTK2, and p38, exhibiting a certain degree of binding affinity. This observation provides molecular-level evidence for the interaction between AS-IV and the ITGB1/PTK2/p38 signaling axis, further supporting the potential of AS-IV as a therapeutic agent for SLE.

The findings of this study demonstrate that AS-IV exerts remarkable anti-inflammatory and immunomodulatory effects, effectively impeding the progression of SLE. AS-IV likely modulates immune cell functions and inflammatory responses by binding to targets within the ITGB1/PTK2/p38 signaling axis, thereby inhibiting their activity and expression. Despite the significant outcomes achieved in this study, there are inherent limitations. Primarily, this research is predominantly grounded in animal experiments. Although MRL/lpr mice are widely recognized as a standard lupus mouse model, the pathogenesis and pathophysiological processes in these animals may deviate from those in human SLE. Consequently, further clinical trials are imperative to validate the efficacy and safety of AS-IV in treating human

SLE. Simultaneously, we intend to integrate cutting-edge technologies such as gene editing and single-cell sequencing. These advanced approaches will enable us to conduct in-depth investigations into the precise regulatory mechanisms of AS-IV on immune cells and signaling pathways. By doing so, we aim to provide a robust theoretical foundation for the development of more effective therapeutic agents for SLE.

## Conclusion

In summary, this study systematically evaluated the efficacy of AS-IV in the treatment of SLE and explored its potential mechanism of action by MRL/lpr mouse model. The results showed that AS-IV could significantly improve renal damage, attenuate immune complex deposition, regulate immune cell function, and reduce inflammatory response, and its therapeutic efficacy was close to that of Pred. Network pharmacology and in vivo experiments further indicated that AS-IV might inhibit immune-inflammatory response by mediating the ITGB1/PTK2/p38 axis, thereby alleviating the progression of SLE. This study not only provides a theoretical basis for the application and molecular mechanism of AS-IV in the treatment of SLE, but also lays the foundation for the clinical application of AS-IV. Further in vitro, in vivo, and clinical studies will be conducted to comprehensively evaluate the efficacy and safety profile of AS-IV, particularly in SLE contexts.

## Data Sharing Statement

Data will be made available on request.

## Ethical Approval

All animal experiments were approved by the Animal Ethics Committee of Anhui University of Traditional Chinese Medicine (No. AHUCM-mouse-2022130). The human data in this study were sourced exclusively from public databases with open licenses permitting unrestricted reuse. Per China's National Science and Technology Ethics Committee guidelines, such data usage is exempt from ethical review (available at https://www.gov.cn/zhengce/zhengceku/2023-02/28/content_5743658.htm). Ethical exemption was confirmed by The First Affiliated Hospital of Anhui University of Chinese Medicine.

## Author Contributions

All authors made a significant contribution to the work reported, whether that is in the conception, study design, execution, acquisition of data, analysis and interpretation, or in all these areas; took part in drafting, revising or critically reviewing the article; gave final approval of the version to be published; have agreed on the journal to which the article has been submitted; and agree to be accountable for all aspects of the work.

## Funding

This study was supported by the National Natural Science Foundation of China (No. 82104782), Clinical Medical Research Transformation Special Project of Anhui Province (No. 202304295107020114 and No. 202304295107020115), and Xin'an Institute of Medicine and Traditional Chinese Medicine Modernization (No.2023CXMMTCM004 and No.2023CXMMTCM015).

## Disclosure

The authors report no conflicts of interest in this work.

## References

1. Avello A, Fernández-Prado R, Abasheva D. et al. Heterogeneity of regional and national hospitalization burden of lupus nephritis and systemic lupus erythematous. *Clin Kidney J*. 2025;18(7):sfaf162. doi:10.1093/ckj/sfaf162
2. Accapezzato D, Caccavale R, Paroli MP, et al. Advances in the Pathogenesis and Treatment of Systemic Lupus Erythematosus. *Int J Mol Sci*. 2023;24(7):6578. doi:10.3390/ijms24076578
3. Moysidou E, Christodoulou M, Lioulios G, et al. Lymphocytes Change Their Phenotype and Function in Systemic Lupus Erythematosus and Lupus Nephritis. *Int J Mol Sci*. 2024;25(20):10905. doi:10.3390/ijms252010905

4. Li H, Boulougoura A, Endo Y, Tsokos GC. Abnormalities of T cells in systemic lupus erythematosus: new insights in pathogenesis and therapeutic strategies. *J Autoimmun*. 2022;132:102870. doi:10.1016/j.jaut.2022.102870
5. Li M, Li C, Cao M, et al. Incidence and prevalence of systemic lupus erythematosus in urban China, 2013-2017: a nationwide population-based study. *Sci Bull*. 2024;69(19):3089–3097. doi:10.1016/j.scib.2024.04.075
6. Perge B, Papp G, Bói B, et al. Prognostic Factors of the Progression of Chronic Kidney Disease and the Development of End-Stage Renal Disease in Patients with Lupus Nephritis: a Retrospective Cohort Study. *J Clin Med*. 2025;14(3):665. doi:10.3390/jcm14030665
7. Li L, Zhang Y, Luo Y, et al. The Molecular Basis of the Anti-Inflammatory Property of Astragaloside IV for the Treatment of Diabetes and Its Complications. *Drug Des Devel Ther*. 2023;17:771–790. doi:10.2147/DDDT.S399423
8. Wei X, Leng X, Liang J, et al. Pharmacological potential of natural medicine Astragali Radix in treating intestinal diseases. *Biomed Pharmacother*. 2024;180:117580. doi:10.1016/j.biopha.2024.117580
9. Liang Y, Chen B, Liang D, et al. Pharmacological Effects of Astragaloside IV: a Review. *Molecules*. 2023;28(16):6118. doi:10.3390/molecules28166118
10. Zhang J, Huang J, Lan J, et al. Astragaloside IV protects against autoimmune myasthenia gravis in rats via regulation of mitophagy and apoptosis. *Mol Med Rep*. 2024;30(1):129. doi:10.3892/mmr.2024.13253
11. Feng M, Lv J, Zhang C, et al. Astragaloside IV Protects Sepsis-induced Acute Kidney Injury by Attenuating Mitochondrial Dysfunction and Apoptosis in Renal Tubular Epithelial Cells. *Curr Pharm Des*. 2022;28(34):2825–2834. doi:10.2174/1381612828666220902123755
12. Gao R, Wu Z, Dang W, et al. Th1/Th2 Immune Imbalance in the Spleen of Mice Induced by Hypobaric Hypoxia Stimulation and Therapeutic Intervention of Astragaloside IV. *Int J Mol Sci*. 2025;26(6):2584. doi:10.3390/ijms26062584
13. Li D, Liu Y, Zhan Q, et al. Astragaloside IV Blunts Epithelial-Mesenchymal Transition and G2/M Arrest to Alleviate Renal Fibrosis via Regulating ALDH2-Mediated Autophagy. *Cells*. 2023;12(13):1777. doi:10.3390/cells12131777
14. Zhang P, Zhang D, Zhou W, et al. Network pharmacology: towards the artificial intelligence-based precision traditional Chinese medicine. *Brief Bioinform*. 2023;25(1):bbad518. doi:10.1093/bib/bbad518
15. Zhao L, Zhang H, Li N, et al. Network pharmacology, a promising approach to reveal the pharmacology mechanism of Chinese medicine formula. *J Ethnopharmacol*. 2023;309:116306. doi:10.1016/j.jep.2023.116306
16. Crampon K, Giorkallos A, Deldossi M, Baud S, Steffenel LA. Machine-learning methods for ligand-protein molecular docking. *Drug Discov Today*. 2022;27(1):151–164. doi:10.1016/j.drudis.2021.09.007
17. Wang R, Yang X, You S, et al. Chlorogenic Acid Relieves the Lupus Erythematosus-like Skin Lesions and Arthritis in MRL/lpr Mice. *Pharmaceuticals (Basel)*. 2022;15(11):1327. doi:10.3390/ph15111327
18. Runz M, Rusche D, Schmidt S, Weihrauch MR, Hesser J, Weis CA. Normalization of HE-stained histological images using cycle consistent generative adversarial networks. *Diagn Pathol*. 2021;16(1):71. doi:10.1186/s13000-021-01126-y
19. de Haan K, Zhang Y, Zuckerman JE, et al. Deep learning-based transformation of H&E stained tissues into special stains. *Nat Commun*. 2021;12(1):4884. doi:10.1038/s41467-021-25221-2
20. Aydin S. A short history, principles, and types of ELISA, and our laboratory experience with peptide/protein analyses using ELISA. *Peptides*. 2015;72:4–15. doi:10.1016/j.peptides.2015.04.012
21. Kim S, Chen J, Cheng T, et al. PubChem in 2021: new data content and improved web interfaces. *Nucleic Acids Res*. 2021;49(D1):D1388–D1395. doi:10.1093/nar/gkaa971
22. Mendez D, Gaulton A, Bento AP, et al. ChEMBL: towards direct deposition of bioassay data. *Nucleic Acids Res*. 2019;47(D1):D930–D940. doi:10.1093/nar/gky1075
23. Daina A, Michielin O, Zoete V. SwissTargetPrediction: updated data and new features for efficient prediction of protein targets of small molecules. *Nucleic Acids Res*. 2019;47(W1):W357–W364. doi:10.1093/nar/gkz382
24. Stelzer G, Rosen N, Plaschkes I, et al. The GeneCards Suite: from Gene Data Mining to Disease Genome Sequence Analyses. *Curr Protoc Bioinform*. 2016;54(1):1.30.1–1.30.33. doi:10.1002/cpbi.5
25. Amberger JS, Hamosh A. Searching Online Mendelian Inheritance in Man (OMIM): a Knowledgebase of Human Genes and Genetic Phenotypes. *Curr Protoc Bioinform*. 2017;58(1):1.2.1–1.2.12. doi:10.1002/cpbi.27
26. Zhou Y, Zhang Y, Zhao D, et al. TTD: therapeutic Target Database describing target druggability information. *Nucleic Acids Res*. 2024;52(D1):D1465–D1477. doi:10.1093/nar/gkad751
27. Piñero J, Ramírez-Anguita JM, Saüch-Pitarch J, et al. The DisGeNET knowledge platform for disease genomics: 2019 update. *Nucleic Acids Res*. 2020;48(D1):D845–D855. doi:10.1093/nar/gkz1021
28. Zhou Y, Zhou B, Pache L, et al. Metascape provides a biologist-oriented resource for the analysis of systems-level datasets. *Nat Commun*. 2019;10(1):1523. doi:10.1038/s41467-019-09234-6
29. Berman HM, Westbrook J, Feng Z, et al. The Protein Data Bank. *Nucleic Acids Res*. 2000;28(1):235–242. doi:10.1093/nar/28.1.235
30. Rua-Figueroa I, Pérez-Veiga N, Rodríguez-Almaraz E, et al. Comorbidity clusters and their relationship with severity and outcomes of index diseases, in a large multicentre systemic lupus erythematosus cohort. *Lupus Sci Med*. 2025;12(2):e001633. doi:10.1136/lupus-2025-001633
31. Mok CC. Immunotargets and Therapy for Systemic Lupus Erythematosus. *Immunotargets Ther*. 2025;14:605–629. doi:10.2147/ITT.S485650
32. Liu YX, Song XM, Dan LW, et al. Astragali Radix: comprehensive review of its botany, phytochemistry, pharmacology and clinical application. *Arch Pharm Res*. 2024;47(3):165–218. doi:10.1007/s12272-024-01489-y
33. Liu N, Ji Y, Liu R, Jin X. The state of astragaloside IV research: a bibliometric and visualized analysis. *Fundam Clin Pharmacol*. 2024;38(2):208–224. doi:10.1111/fcp.12956
34. Menon R, Bomback AS, Lake BB, et al. Integrated single-cell sequencing and histopathological analyses reveal diverse injury and repair responses in a participant with acute kidney injury: a clinical-molecular-pathologic correlation. *Kidney Int*. 2022;101(6):1116–1125. doi:10.1016/j.kint.2022.03.011
35. Rastin M, Mahmoudi M, Sahebari M, Tabasi N. Clinical & immunological characteristics in systemic lupus erythematosus patients. *Indian J Med Res*. 2017;146(2):224–229. doi:10.4103/ijmr.IJMR_1356_15
36. Lee AYS. IgA anti-dsDNA antibodies: a neglected serological parameter in systemic lupus erythematosus. *Lupus*. 2022;31(2):137–142. doi:10.1177/09612033221074184

37. Andrianova IA, Ponomareva AA, Mordakhanova ER, et al. In systemic lupus erythematosus anti-dsDNA antibodies can promote thrombosis through direct platelet activation. *J Autoimmun*. 2020;107:102355. doi:10.1016/j.jaut.2019.102355
38. Li C, Ma A, Bai Y, et al. TRIM21 promotes type I interferon by inhibiting the autophagic degradation of STING via p62/SQSTM1 ubiquitination in systemic lupus erythematosus. *Acta Biochim Biophys Sin (Shanghai)*. 2025;57(5):834–846. doi:10.3724/abbs.2025046
39. Gao M, Liu S, Chatham WW, Mountz JD, Hsu HC. IL-4-Induced Quiescence of Resting Naive B Cells Is Disrupted in Systemic Lupus Erythematosus. *J Immunol*. 2022;209(8):1513–1522. doi:10.4049/jimmunol.2200409
40. Liu Y, Zhang Z, Kang Z, et al. Interleukin 4-driven reversal of self-reactive B cell anergy contributes to the pathogenesis of systemic lupus erythematosus. *Ann Rheum Dis*. 2023;82(11):1444–1454. doi:10.1136/ard-2023-224453
41. Espinoza-García N, Salazar-Camarena DC, Marín-Rosales M, et al. High Interleukin 21 Levels in Patients with Systemic Lupus Erythematosus: association with Clinical Variables and rs2221903 Polymorphism. *J Clin Med*. 2024;13(15):4512. doi:10.3390/jcm13154512
42. Ding L, Wang S, Chen GM, Leng RX, Pan HF, Ye DQ. A single nucleotide polymorphism of IL-21 gene is associated with systemic lupus erythematosus in a Chinese population. *Inflammation*. 2012;35(6):1781–1785. doi:10.1007/s10753-012-9497-7
43. Huangfu L, Li R, Huang Y, Wang S. The IL-17 family in diseases: from bench to bedside. *Signal Transduct Target Ther*. 2023;8(1):402. doi:10.1038/s41392-023-01620-3
44. Ebrahimi Chaharom F, Ebrahimi AA, Feghhi Koochebagh F, et al. Association of IL-17 serum levels with clinical findings and systemic lupus erythematosus disease activity index. *Immunol Med*. 2023;46(4):175–181. doi:10.1080/25785826.2023.2202050
45. Zhong W, Feng L, Tian W, et al. SMURF1 inhibits the Th17 and Th17.1 polarization and improves the Treg/Th17 imbalance in systemic lupus erythematosus through the ubiquitination of RORγt. *Mol Immunol*. 2023;157:186–194. doi:10.1016/j.molimm.2023.03.024
46. Gu W, Sun H, Zhang M, et al. ITGB1 as a prognostic biomarker correlated with immune suppression in gastric cancer. *Cancer Med*. 2023;12 (2):1520–1531. doi:10.1002/cam4.5042
47. Khawaja AA, Pericleous C, Ripoll VM, Porter JC, Giles IP. Autoimmune rheumatic disease IgG has differential effects upon neutrophil integrin activation that is modulated by the endothelium. *Sci Rep*. 2019;9(1):1283. doi:10.1038/s41598-018-37852-5
48. Chen Z, Zhao H, Meng L, Yu S, Liu Z, Xue J. Microfibril-Associated Glycoprotein-2 Promoted Fracture Healing via Integrin αvβ3/PTK2/AKT Signaling. *Lab Invest*. 2023;103(7):100121. doi:10.1016/j.labinv.2023.100121
49. Nakayamada S, Saito K, Nakano K, Tanaka Y. Activation signal transduction by beta1 integrin in T cells from patients with systemic lupus erythematosus. *Arthritis Rheum*. 2007;56(5):1559–1568. doi:10.1002/art.22581
50. Siyang W, Xia H, Pinhu L. Potential diagnostic biomarkers and Mapk14 protein expression: autophagy-related genes linking immune infiltration in acute respiratory distress syndrome. *Int J Biol Macromol*. 2024;279(Pt 1):135077. doi:10.1016/j.ijbiomac.2024.135077
51. Cambier S, Gouwy M, Proost P. The chemokines CXCL8 and CXCL12: molecular and functional properties, role in disease and efforts towards pharmacological intervention. *Cell Mol Immunol*. 2023;20(3):217–251. doi:10.1038/s41423-023-00974-6
52. Han B, Sun C, Yang R, et al. Dihydrotanshinone I inhibits ovarian tumor growth by suppressing ITGB1/FAK-mediated extracellular matrix signaling. *Phytomedicine*. 2025;2025:157023. doi:10.1016/j.phymed.2025.157023
53. Zhang X, Li P, Zhou J, et al. FAK-p38 signaling serves as a potential target for reverting matrix stiffness-modulated liver sinusoidal endothelial cell defenestration. *Biomaterials*. 2024;305:122462. doi:10.1016/j.biomaterials.2023.122462